

Keynote Paper

Smart system identification of super high-rise buildings using limited vibration data during the 2011 Tohoku earthquake

I. Takewaki¹⁾

*Department of Architecture and Architectural Engineering, Kyoto University
Kyotodaigaku-Katsura, Nishikyo-ku, Kyoto 615-8540, Japan
takewaki@archi.kyoto-u.ac.jp*

ABSTRACT

A new method of smart system identification of super high-rise buildings is proposed in which super high-rise buildings are represented by a shear-bending model. The method is aimed at finding the story shear and bending stiffnesses of a specific story only from the horizontal floor accelerations. The special characteristic of the proposed method is to use a previously derived set of closed-form expressions for the story shear and bending stiffnesses in terms of the limited floor accelerations and to utilize a reduced shear-bending model with the same number of elements as the vibration recording points. In the proposed method, a difficulty of prediction of an unstable specific function in a low frequency range can be overcome by introducing an ARX model. It is demonstrated that the shear-bending model can simulate the vibration records with a reasonable accuracy. It is shown further that the vibration records at two super high-rise buildings during the 2011 Tohoku (Japan) earthquake can be simulated with the proposed method including a technique of adding degrees of freedom between the vibration recording points.

Keywords: System identification, Structural health monitoring, Shear-bending model, High-rise building, ARX model, 2011 Tohoku earthquake

¹⁾ Professor

1. Introduction

The 2011 off the Pacific coast of Tohoku earthquake (Tohoku earthquake) induced intensive vibration of peculiar character in super high-rise buildings in Japan (Tokyo, Nagoya and Osaka) for the first time after the construction of such super high-rise buildings. Unfortunately, such vibration characteristics were not taken into account in the design stage of super high-rise buildings. This earthquake is also thought to be the largest one after the 1923 Great Kanto earthquake (Takewaki et al. 2011a, Kasai et al. 2012, Hisada et al. 2012) which affected the wide area of mega cities in Japan. It seems important to analyze the vibration characteristics of super high-rise buildings for future directions of structural design of super high-rise buildings.

A great deal of interest is focused recently on system identification corresponding to the increasing need for damage detection of building structures under or after earthquakes (Hart and Yao 1977, Beck and Jennings 1980, Hoshiya and Saito 1984, KOzin and Natke 1986, Agbabian et al. 1991, Koh et al. 1991, Yao and Natke 1994, Housner et al. 1994, Hjelmstad et al. 1995, Ghanem and Shinozuka 1995, Shinozuka and Ghanem 1995, Masri et al. 1996, Doebling et al. 1996, Hjelmstad 1996, Housner et al. 1997, Kobori et al. 1998, Casciati 2002, Bernal and Beck 2004, Lus et al. 2004, Johnson and Smyth 2006, Nagarajaiah and Basu 2009, Fujino et al. 2010, Ji et al. 2011). Such need of damage detection stems from the accelerated demand of rapid assessment for continuing use of buildings (business continuity planning) after earthquakes. The recognition of actual phenomena and the elucidation of underlying properties are very important for the reliable system identification and damage detection and should be supported by the investigation on actual data and related theories. Filling and narrowing the gap between actual data and the corresponding theories enabled one to accelerate the advancement of the research in this field (Safak 1995, Celebi 1996, Beck 2004, Stewart and Fenves 1998, Lus et al. 1999, Naeim 2000, Dunand et al. 2006, Nayeri et al. 2008, Yang and Nagarajaiah 2012). A comprehensive review of system identification and damage detection has been provided (Kerschen et al. 2006, Nagarajaiah and Basu 2009, Lee et al. 2010). It is also well-recognized that system identification plays an important role in filling gaps between the constructed structural and infrastructural systems and their structural design models (model refinement) and sophisticating the modeling technique to be able to describe the structural behaviors in a more accurate and reliable manner.

Modal parameter system identification is well-established and a versatile research has been accumulated (for example Hart and Yao 1977, Beck and Jennings 1980, Safak 1989, Takewaki et al. 2011b). In the modal parameter system identification, observation at two places is necessary for natural frequency and damping ratio identification. On the other hand, observation at many points is usually required for modal shape identification. It is believed that this often requires a cumbersome task.

In contrast to such modal parameter system identification, the research on physical parameter system identification is scarce and has been developed for direct identification of physical parameters (stiffness and damping coefficients). For example, Takewaki and Nakamura (2000, 2005) introduced a method based on the mathematically eminent work by Udwadia et al. (1978). In that method, a shear building model is used and stiffness and damping coefficients of a specific story are identified

directly from the floor accelerations just above and below the specific story. However the method by Takewaki and Nakamura (2000, 2005) has a difficulty resulting from the small signal/noise (SN) ratio in the low frequency range and cannot be applied to high-rise buildings with large aspect ratios (height/width ratio). Independently Hernandez-Garcia et al. (2010a, b) have developed an interesting method of damage detection using a floor-by-floor approach to enhance the efficiency and accuracy of the identification results.

Furthermore a combined method of the modal parameter system identification and the physical parameter system identification is also well used (for example Hjelmstad et al. 1995, Barroso and Rodriguez 2004). After modal parameters are identified in a stable manner, physical parameters are determined by solving inverse problems.

The number of sensor locations in a building structure is usually limited because of the cost and functionality disturbance problems. The problem of optimal sensor locations and data interpolation is therefore getting much interest recently (Shah and Udwadia 1978, Udwadia 1994, Heredia-Zavoni and Esteva 1998, Worden and Burrows 2001, Limongelli 2003, Papadimitriou 2004, Yi et al. 2011, Limongelli 2005, Goel 2008, Yoshitomi et al. 2010, Takewaki et al. 2011b). While a few sensor locations enable the identification of natural periods (lowest few) and the maximum response level of such locations in general, it is desired that more detailed structural properties are identified by constructing even reduced structural models (shear models, shear-bending models, etc).

In this paper, a system identification method for high-rise buildings is proposed by introducing a shear-bending model which can describe the overall bending behavior, stemming from column elongation, of such high-rise buildings. While most of the previous methods are based on a shear model and modal identification approaches are often used, a physical-parameter approach, even using a few masses due to the limitation of recording points, is introduced. It is demonstrated that the shear-bending model can simulate the vibration records with a reasonable accuracy. It is shown further that the vibration records at two super high-rise buildings during the 2011 Tohoku (Japan) earthquake can be simulated with the proposed method including a technique of adding degrees of freedom between the vibration recording points. Inclusion of higher modes in the previous modal approaches seems to have difficulties in the accuracy of identification of higher modes. After an average identification, a further approach for capturing the time-varying mechanical characteristics of a building is proposed.

The above-mentioned difficulty arising in the limit manipulation in the method by Takewaki and Nakamura (2000, 2005) is overcome by introducing an ARX model as in the References (Kuwabara et al. 2012, Maeda et al. 2011). The weakness of a small SN ratio in the low frequency range in the method (Takewaki and Nakamura 2000, 2005) is avoided by using the ARX model. Another difficulty due to large aspect ratios is tackled by introducing a shear-bending model introduced in the Reference (Kuwabara et al. 2012). The validity of the method is examined through numerical examples for an assumed building and actual buildings.

2. Governing equations and identification function

2.1. Shear-bending model and equations of motion

Consider an N -story shear-bending building model as shown in Fig.1(a). Every story of this shear-bending model consists of a rotational spring and an extensional spring. These two springs are connected in series. Let k_{sj} and k_{bj} denote the stiffness of the extensional spring and that of the rotational spring, respectively. As for damping, let c_{sj} and c_{bj} denote the damping coefficient of the extensional dashpot and that of the rotational dashpot, respectively. These two dashpots are also connected in series as in springs. The floor mass and its rotational mass moment of inertia are denoted by m_j and J_j , respectively. The story height of the j -th story is given by H_j .

Let \mathbf{M} , \mathbf{K} and \mathbf{C} denote the mass, stiffness and damping matrices of this shear-bending building model and let y_j and θ_j denote the horizontal i -th floor displacement and the angle of i -th floor rotation, respectively. The set of floor displacements and angles of rotation relative to base is denoted by \mathbf{u} . The equations of motion for this model subjected to a horizontal ground acceleration \ddot{u}_g can be expressed as

$$\mathbf{M}\ddot{\mathbf{u}} + \mathbf{C}\dot{\mathbf{u}} + \mathbf{K}\mathbf{u} = -\mathbf{M}\mathbf{r}\ddot{u}_g \quad (1)$$

where

$$\mathbf{M} = \text{diag}(m_1, \dots, m_N \mid J_1, \dots, J_N)$$

$$\mathbf{C} = \begin{bmatrix} \mathbf{C}_{HH} & \mathbf{C}_{HR} \\ \mathbf{C}_{HR}^T & \mathbf{C}_{RR} \end{bmatrix}, \quad \mathbf{K} = \begin{bmatrix} \mathbf{K}_{HH} & \mathbf{K}_{HR} \\ \mathbf{K}_{HR}^T & \mathbf{K}_{RR} \end{bmatrix}$$

$$\mathbf{K}_{HH} = \begin{bmatrix} k_{s1} + k_{s2} & -k_{s2} & & \mathbf{0} \\ -k_{s2} & \ddots & \ddots & \\ & \ddots & k_{sN-1} + k_{sN} & -k_{sN} \\ \mathbf{0} & & -k_{sN} & k_{sN} \end{bmatrix}, \quad \mathbf{K}_{HR} = \begin{bmatrix} -H_1 k_{s1} & H_2 k_{s2} & & \mathbf{0} \\ 0 & \ddots & \ddots & \\ & \ddots & \ddots & H_N k_{sN} \\ \mathbf{0} & & 0 & -H_N k_{sN} \end{bmatrix},$$

$$\mathbf{K}_{RR} = \begin{bmatrix} H_1^2 k_{s1} + k_{b1} + k_{b2} & -k_{b2} & & \mathbf{0} \\ -k_{b2} & \ddots & \ddots & \\ & \ddots & \ddots & -k_{bN} \\ \mathbf{0} & & -k_{bN} & H_N^2 k_{sN} + k_{bN} \end{bmatrix}$$

$$\mathbf{u} = \{y_1, \dots, y_N \mid \theta_1, \dots, \theta_N\}^T$$

$$\mathbf{r} = \{1, \dots, 1 \mid 0, \dots, 0\}^T \quad (2a-h)$$

The sub damping matrices \mathbf{C}_{HH} , \mathbf{C}_{HR} , \mathbf{C}_{RR} can be derived by replacing k_{si} and k_{bi}

with c_{si} and c_{bi} in the sub stiffness matrices $\mathbf{K}_{HH}, \mathbf{K}_{HR}, \mathbf{K}_{RR}$.

2.2. Dynamic equilibrium in frequency domain

Let v_j and ϕ_j denote the shear deformation (elongation of the extensional spring) and the bending deformation (angle of rotation of the rotational spring), respectively. Then v_j and ϕ_j can be expressed in terms of y_j and θ_j .

$$v_j = y_j - y_{j-1} - \theta_j H_j \quad (3a)$$

$$\phi_j = \theta_j - \theta_{j-1} \quad (3b)$$

From the dynamic equilibrium of a free body shown in Fig.1(b), the following equations can be derived.

$$k_{sj}v_j + c_{sj}\dot{v}_j = \sum_{i=j}^N \{-m_i(\ddot{u}_g + \ddot{y}_i)\} \quad (4a)$$

$$k_{bj}\phi_j + c_{bj}\dot{\phi}_j = \sum_{i=j}^N \{-m_i(\ddot{u}_g + \ddot{y}_i)(H_i^t - H_{j-1}^t)\} + \sum_{i=j}^N (-J_i\ddot{\theta}_i) \quad (4b)$$

where $H_i^t = \sum_{j=1}^i H_j$. It will be assumed later that the second term in the right-hand side of Eq.(4b) can be neglected compared to the first term. It was shown in the Reference (Kuwabara et al. 2012) that Fourier transformation of Eqs.(3a,b) and (4a,b) and arrangement of the resulting equations lead to

$$\frac{1}{k_{sj} + i\omega c_{sj}} \cdot \frac{-\omega^2 \sum_{i=j}^N \{-m_i(\ddot{U}_g + \ddot{Y}_i)\}}{\{\ddot{U}_g + \ddot{Y}_j - (\ddot{U}_g + \ddot{Y}_{j-1})\}} - \omega^2 H_j \sum_{m=1}^j \left[\frac{1}{k_{bm} + i\omega c_{bm}} \frac{\sum_{i=m}^N \{-m_i(H_i^t - H_{m-1}^t)(\ddot{U}_g + \ddot{Y}_i)\}}{\{\ddot{U}_g + \ddot{Y}_j - (\ddot{U}_g + \ddot{Y}_{j-1})\}} \right] = 1 \quad (5)$$

In Eq.(5), \ddot{U}_g, \ddot{Y}_j are Fourier transforms of \ddot{u}_g, \ddot{y}_j , respectively. The derivation of Eq.(5) plays a central role in the system identification using the shear-bending model.

After some manipulations, the bending (rotational) and shear (extensional) stiffnesses have been derived in the Reference (Kuwabara et al. 2012) with the stiffness ratio $R_j = k_{bj}/k_{sj}$.

$$k_{bj} = \frac{R_j + \frac{H_j}{\sum_{i=j}^N m_i} \sum_{i=j}^N \{m_i (H_i^t - H_{j-1}^t)\}}{\lim_{\omega \rightarrow 0} \left[\text{Re} \{F_j(\omega)\} \right] - \frac{H_j}{\sum_{i=j}^N m_i} \sum_{m=1}^{j-1} \left[\frac{\sum_{i=m}^N \{m_i (H_i^t - H_{m-1}^t)\}}{k_{bm}} \right]} \quad (6a)$$

$$k_{sj} = k_{bj} / R_j \quad (6b)$$

where $F_j(\omega)$ is called 'an identification function' and is defined by

$$F_j(\omega) = \left(\frac{\ddot{U}_g + \ddot{Y}_{j-1}}{\ddot{U}_g + \ddot{Y}_j} - 1 \right) \left/ \left(-\omega^2 \sum_{i=j}^N m_i \right) \right. \quad (6c)$$

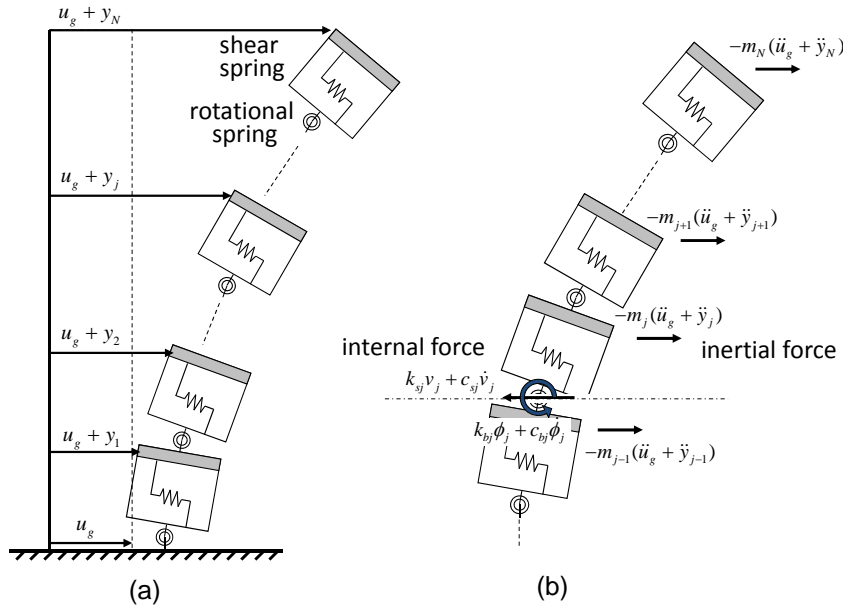


Fig.1 (a) Shear-bending model, (b) Dynamic equilibrium of free body above j -th story

3. Identification method 1 (Transfer function matching)

Let us introduce the following transfer function (j -th-story horizontal acceleration to $(j-1)$ -th-story acceleration) in analogy from shear building models (Takewaki and Nakamura 2000):

$$G_j = \frac{\ddot{U}_g + \ddot{Y}_j}{\ddot{U}_g + \ddot{Y}_{j-1}} \quad (7)$$

Rewriting Eq.(5) using the transfer function of Eq.(7) with a further definition $GG(j) = \prod_{k=1}^j G_k$ leads to

$$\begin{aligned} & \frac{-\omega^2}{k_{sj} + i\omega c_{sj}} \sum_{i=j}^N \frac{m_i GG(i)}{GG(j-1) - GG(j)} \\ & - \frac{H_j}{GG(j-1) - GG(j)} \sum_{i=1}^j \left[\frac{\omega^2}{k_{bi} + i\omega c_{bi}} \sum_{l=i}^N \left\{ m_l GG(l) \sum_{k=i}^l H_k \right\} \right] = 1 \end{aligned} \quad (8)$$

It can be shown that the $(j-1)$ th-story transfer function can be expressed in terms of the transfer functions from the j th through the N th story. Equation (8) for the j th story can be applied to $(j-1)$ th story. By dividing Eq.(8) for $(j-1)$ th story by a quantity $H_{j-1} / \{GG(j-2) - GG(j-1)\}$, the following relation can be obtained.

$$\begin{aligned} & \sum_{i=1}^{j-1} \left[\frac{\omega^2}{k_{bi} + i\omega c_{bi}} \sum_{l=i}^N \left\{ m_l GG(l) \sum_{k=i}^l H_k \right\} \right] \\ & = \frac{GG(j-2) - GG(j-1)}{H_{j-1}} \left\{ \frac{-\omega^2}{k_{sj-1} + i\omega c_{sj-1}} \sum_{i=j-1}^N \frac{m_i GG(i)}{GG(j-2) - GG(j-1)} - 1 \right\} \end{aligned} \quad (9)$$

Application of Eq.(9) to the second term of the left-hand side in Eq.(8) provides the following expression after lengthy manipulation.

$$\begin{aligned} G_{j-1} = 1 / & \left[1 + \frac{H_{j-1}(1-G_j)}{H_j} \left\{ 1 + \frac{\omega^2}{k_{sj} + i\omega c_{sj}} \sum_{i=j}^N \frac{m_i GG(i)}{GG(j-1) - GG(j)} \right. \right. \\ & \left. \left. + \frac{\omega^2}{k_{bj} + i\omega c_{bj}} H_j \sum_{l=j}^N \frac{m_l GG(l) \sum_{k=j}^l H_k}{GG(j-1) - GG(j)} - \frac{H_j}{H_{j-1}} \frac{\omega^2}{k_{sj-1} + i\omega c_{sj-1}} \sum_{i=j-1}^N \frac{m_i GG(i)}{GG(j-1) - GG(j)} \right\} \right] \end{aligned} \quad (10)$$

The terms in Eq.(10) can be expressed as follows by the transfer function from the j th through the N th story.

$$\sum_{i=j}^N \frac{GG(i)}{GG(j-1) - GG(j)} = \frac{G_j + G_{j+1}G_j + G_{j+2}G_{j+1}G_j + \dots}{1 - G_j} \quad (11a)$$

$$\sum_{i=j-1}^N \frac{GG(i)}{GG(j-1) - GG(j)} = \frac{1 + G_j + G_{j+1}G_j + \dots}{1 - G_j} \quad (11b)$$

It should be noted that G_{j-1} in Eq.(10) is a function of $\{R_j\}$. Assume $\{R_j\}$ first and G_N is computed from the records. Then the correspondence between $G_j(\omega, R_j)$

in terms of $\{R_j\}$ and $G_j(\text{record})$ ($j=N-1, \dots, 1$) is considered. $\{R_j\}$ can be determined by applying the least-squares method (for many frequencies) to G_{j-1} in Eq.(10) and the transfer function derived from records by the ARX model. The flowchart of the identification method 1 is shown in Fig.2.

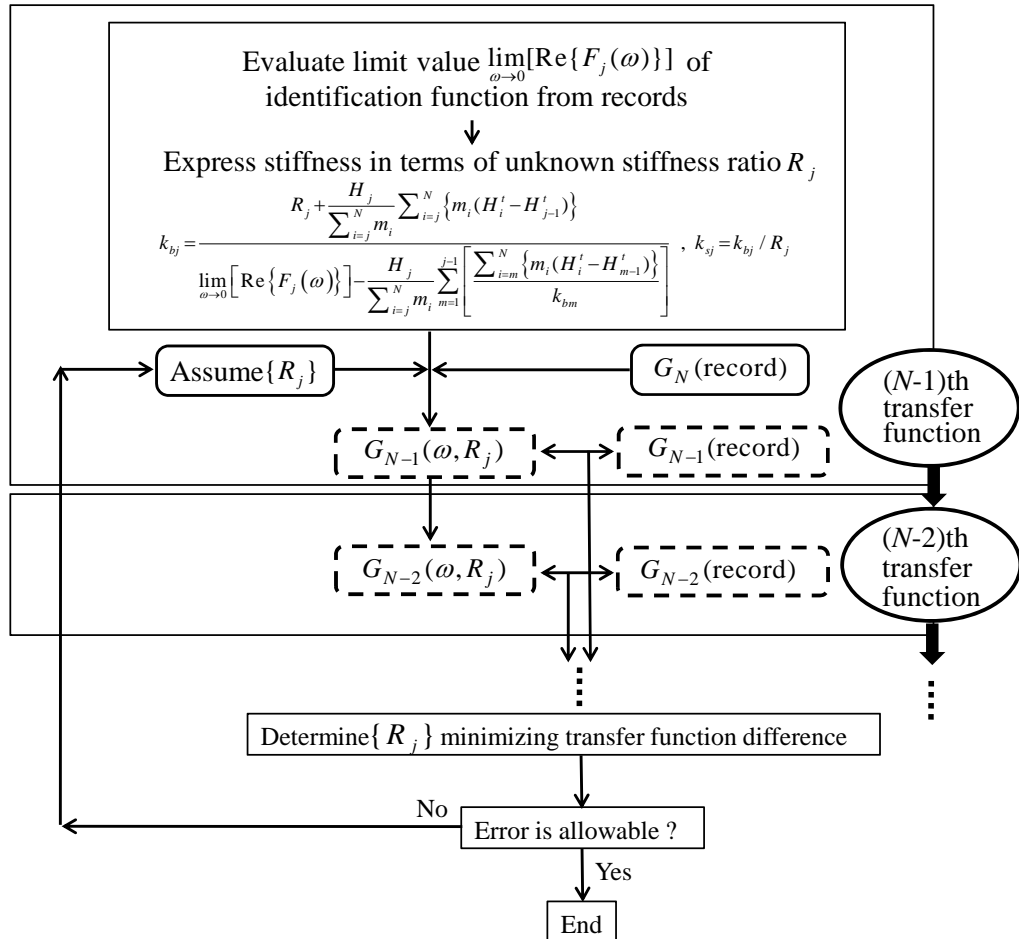


Fig.2 Flowchart of identification method 1

4. Identification method 1 (Equilibrium guarantee)

4.1 Elimination of rotational degrees of freedom

Consider again the equations of motion, Eq.(1), for the shear-bending model subjected to the horizontal base acceleration. Recall the decomposition of the stiffness matrix in Eq.(2c). Then neglect of the rotational inertia forces and damping forces compared to the stiffness terms leads to

$$\mathbf{K}_{HR}^T \mathbf{y} + \mathbf{K}_{RR} \boldsymbol{\theta} = \mathbf{0} \quad (12)$$

Elimination of the angle of rotation in the horizontal equilibrium provides

$$\bar{\mathbf{M}}\ddot{\mathbf{u}}(t) + \bar{\mathbf{C}}\dot{\mathbf{u}}(t) + \bar{\mathbf{K}}\mathbf{u}(t) = -\bar{\mathbf{M}}\mathbf{1}\ddot{u}_g(t) \quad (13)$$

where

$$\bar{\mathbf{K}} = \mathbf{K}_{HH} - \mathbf{K}_{HR}\mathbf{K}_{RR}^{-1}\mathbf{K}_{HR}^T \quad (14)$$

$$\bar{\mathbf{C}} = \text{reduced damping matrix} \quad (15)$$

$$\bar{\mathbf{M}} = \text{diag}(m_1, \dots, m_N) \quad (16)$$

$$\mathbf{u}(t) = \{y_1, \dots, y_N\}^T, \quad \mathbf{1} = \{1, \dots, 1\}^T \quad (17a, b)$$

4.2 Determination of stiffness matrix components by minimization of un-equilibrium forces in horizontal direction

Denote the general stiffness and damping matrices by

$$\bar{\mathbf{K}}^* = \begin{bmatrix} k_{11} & k_{12} & \cdots & k_{1N} \\ k_{21} & k_{22} & & \\ \vdots & & \ddots & \vdots \\ k_{N1} & & \cdots & k_{NN} \end{bmatrix}, \quad \bar{\mathbf{C}}^* = \begin{bmatrix} c_{11} & c_{12} & \cdots & c_{1N} \\ c_{21} & c_{22} & & \\ \vdots & & \ddots & \vdots \\ c_{N1} & & \cdots & c_{NN} \end{bmatrix} \quad (18a, b)$$

The equilibrium of the j th story in the horizontal direction may be expressed by

$$\begin{aligned} c_{j1}\dot{y}_1 + c_{j2}\dot{y}_2 + \cdots + c_{jN}\dot{y}_N \\ + k_{j1}y_1 + k_{j2}y_2 + \cdots + k_{jN}y_N = -m_j(\ddot{y}_j + \ddot{u}_g) \end{aligned} \quad (19)$$

The process of minimizing the un-equilibrium forces obtained in Eq.(19) by substituting the records $\{y_i\}, \{\dot{y}_i\}, \{\ddot{y}_i\}$ plays a key role and is explained next. The minimization (stationarity) conditions can be described as follows by multiplying \dot{y}_i and y_i on Eq.(19) for all masses and all time steps.

$$\begin{aligned} c_{j1}\dot{y}_1\dot{y}_i + c_{j2}\dot{y}_2\dot{y}_i + \cdots + c_{ji}\dot{y}_i^2 + \cdots + c_{jN}\dot{y}_i\dot{y}_N \\ + k_{j1}y_1\dot{y}_i + k_{j2}y_2\dot{y}_i + \cdots + k_{jN}y_N\dot{y}_i = -m_j(\ddot{y}_j + \ddot{u}_g)\dot{y}_i \end{aligned} \quad (20)$$

$$\begin{aligned} c_{j1}y_i\dot{y}_1 + c_{j2}y_i\dot{y}_2 + \cdots + c_{jN}y_i\dot{y}_N \\ + k_{j1}y_1y_i + k_{j2}y_2y_i + \cdots + k_{ji}y_i^2 + \cdots + k_{jN}y_iy_N = -m_j(\ddot{y}_j + \ddot{u}_g)y_i \end{aligned} \quad (21)$$

Eqs.(20), (21) for all time steps ($t_1 \leq t \leq t_e$) can be arranged in a compact form.

$$\left[\bar{\mathbf{K}}^* \mid \bar{\mathbf{C}}^* \right] \mathbf{H}^T \mathbf{H} = -\bar{\mathbf{M}} \mathbf{Z} \mathbf{H} \quad (22)$$

where

$$\mathbf{H} = \left[\begin{array}{ccc|ccc} y_1(t_1) & \cdots & y_N(t_1) & \dot{y}_1(t_1) & \cdots & \dot{y}_N(t_1) \\ \vdots & & \vdots & \vdots & & \vdots \\ y_1(t_e) & \cdots & y_N(t_e) & \dot{y}_1(t_e) & \cdots & \dot{y}_N(t_e) \end{array} \right] \quad (23)$$

$$\mathbf{Z} = \left[\begin{array}{ccc|ccc} \ddot{y}_1(t_1) + \ddot{u}_g(t_1) & \cdots & \ddot{y}_N(t_1) + \ddot{u}_g(t_1) \\ \vdots & & \vdots \\ \ddot{y}_1(t_e) + \ddot{u}_g(t_e) & \cdots & \ddot{y}_N(t_e) + \ddot{u}_g(t_e) \end{array} \right]^T \quad (24)$$

For brevity of expression, the matrices in Eqs.(23), (24) can be expressed as

$$\mathbf{H} = [\mathbf{y}_1 \quad \cdots \quad \mathbf{y}_N \mid \dot{\mathbf{y}}_1 \quad \cdots \quad \dot{\mathbf{y}}_N] \quad (25)$$

$$\mathbf{Z} = [\ddot{\mathbf{u}}_1 \quad \cdots \quad \ddot{\mathbf{u}}_N]^T \quad (26)$$

where

$$\mathbf{y}_j = \{y_j(t_1) \quad \cdots \quad y_j(t_e)\}^T \quad (27a)$$

$$\dot{\mathbf{y}}_j = \{\dot{y}_j(t_1) \quad \cdots \quad \dot{y}_j(t_e)\}^T \quad (27b)$$

$$\ddot{\mathbf{u}}_j = [\ddot{y}_j(t_1) + \ddot{u}_g(t_1) \quad \cdots \quad \ddot{y}_j(t_e) + \ddot{u}_g(t_e)]^T \quad (27c)$$

By post-multiplying $(\bar{\mathbf{H}}^T \bar{\mathbf{H}})^{-1}$ on Eq.(22), the stiffness and damping matrices can be obtained as

$$\left[\bar{\mathbf{K}}^* \mid \bar{\mathbf{C}}^* \right] = -\bar{\mathbf{M}} \mathbf{Z} \mathbf{H} (\mathbf{H}^T \mathbf{H})^{-1} \quad (28)$$

It should be noted that the symmetricity condition for the stiffness and damping matrices is not introduced. By applying this symmetricity condition, the following relation is derived.

$$\mathbf{H}_1 \mathbf{H}_2 \begin{Bmatrix} \mathbf{k} \\ \mathbf{c} \end{Bmatrix} = -\mathbf{H}_1 \mathbf{H}_3 \mathbf{m} \quad (29)$$

where

$$\mathbf{k} = \{k_{11} \quad \cdots \quad k_{1N} \quad k_{22} \quad \cdots \quad k_{2N} \quad \cdots \quad k_{NN}\}^T \quad (30a)$$

$$\mathbf{c} = \{c_{11} \quad \cdots \quad c_{1N} \quad c_{22} \quad \cdots \quad c_{2N} \quad \cdots \quad c_{NN}\}^T \quad (30b)$$

$$\mathbf{m} = \{m_1 \quad \cdots \quad m_N\}^T \quad (30c)$$

$$\mathbf{H}_1 = \left[\begin{array}{cccc|cccc} \mathbf{y}_1 & & \mathbf{0} & & \mathbf{y}_N & & \mathbf{0} & & \dot{\mathbf{y}}_1 & & \mathbf{0} & & \dot{\mathbf{y}}_N & & \mathbf{0} \\ & \ddots & & & & \ddots & & & & \ddots & & & & \ddots & \\ \mathbf{0} & & \mathbf{y}_1 & & \mathbf{0} & & \mathbf{y}_N & & \mathbf{0} & & \dot{\mathbf{y}}_1 & & \mathbf{0} & & \dot{\mathbf{y}}_N \end{array} \right]^T \quad (30d)$$

$$\mathbf{H}_2 = \left[\begin{array}{cccccccc|cccccccc} \mathbf{y}_1 & \mathbf{y}_2 & \cdots & \cdots & \mathbf{y}_N & & & & & & & & & & & & \mathbf{0} \\ & \mathbf{y}_1 & \mathbf{0} & \cdots & \mathbf{0} & \mathbf{y}_2 & \mathbf{y}_3 & \cdots & \cdots & \mathbf{y}_N & & & & & & & \\ & & \mathbf{y}_1 & \mathbf{0} & \cdots & \mathbf{0} & \mathbf{y}_2 & \mathbf{0} & \cdots & \mathbf{0} & \mathbf{y}_3 & \cdots & \mathbf{y}_N & & & & \\ & & & \ddots & & & & \ddots & & & & & & \ddots & & & \\ \mathbf{0} & & & & \mathbf{y}_1 & & & & & & & & & & & & \mathbf{y}_N \end{array} \right] \quad (30e)$$

$$\left[\begin{array}{cccccccc|cccccccc} \dot{\mathbf{y}}_1 & \dot{\mathbf{y}}_2 & \cdots & \cdots & \dot{\mathbf{y}}_N & & & & & & & & & & & & \mathbf{0} \\ & \dot{\mathbf{y}}_1 & \mathbf{0} & \cdots & \mathbf{0} & \dot{\mathbf{y}}_2 & \dot{\mathbf{y}}_3 & \cdots & \cdots & \dot{\mathbf{y}}_N & & & & & & & \\ & & \dot{\mathbf{y}}_1 & \mathbf{0} & \cdots & \mathbf{0} & \dot{\mathbf{y}}_2 & \mathbf{0} & \cdots & \mathbf{0} & \dot{\mathbf{y}}_3 & \cdots & \dot{\mathbf{y}}_N & & & & \\ & & & \ddots & & & & \ddots & & & & & & \ddots & & & \\ \mathbf{0} & & & & \dot{\mathbf{y}}_1 & & & & & & & & & & & & \dot{\mathbf{y}}_N \end{array} \right]$$

$$\mathbf{H}_3 = \left[\begin{array}{ccc} \ddot{\mathbf{u}}_1 & & \mathbf{0} \\ & \ddots & \\ \mathbf{0} & & \ddot{\mathbf{u}}_N \end{array} \right] \quad (30f)$$

By pre-multiplying $(\mathbf{H}_1\mathbf{H}_2)^{-1}$ on Eq.(29), the following stiffness and damping matrices components can be obtained.

$$\begin{Bmatrix} \mathbf{k} \\ \mathbf{c} \end{Bmatrix} = -(\mathbf{H}_1\mathbf{H}_2)^{-1} \mathbf{H}_1\mathbf{H}_3\mathbf{m} \quad (31)$$

\mathbf{H}_1 and \mathbf{H}_2 are not square matrices and further development of matrix multiplication cannot be applied. This is a kind of inverse problems for given response time histories (displacement, velocity and acceleration). The components of $\bar{\mathbf{K}}$ in Eq. (14) is a function of $\{R_j\}$. $\{R_j\}$ can then be determined by applying the regular least-squares method to $\bar{\mathbf{K}}$ in Eq.(14) and $\bar{\mathbf{K}}^*$ in Eqs.(18) and (31). The introduction of the symmetricity condition on the stiffness and damping matrices may be a new

addition. The flowchart of the identification method 2 is shown in Fig.3.

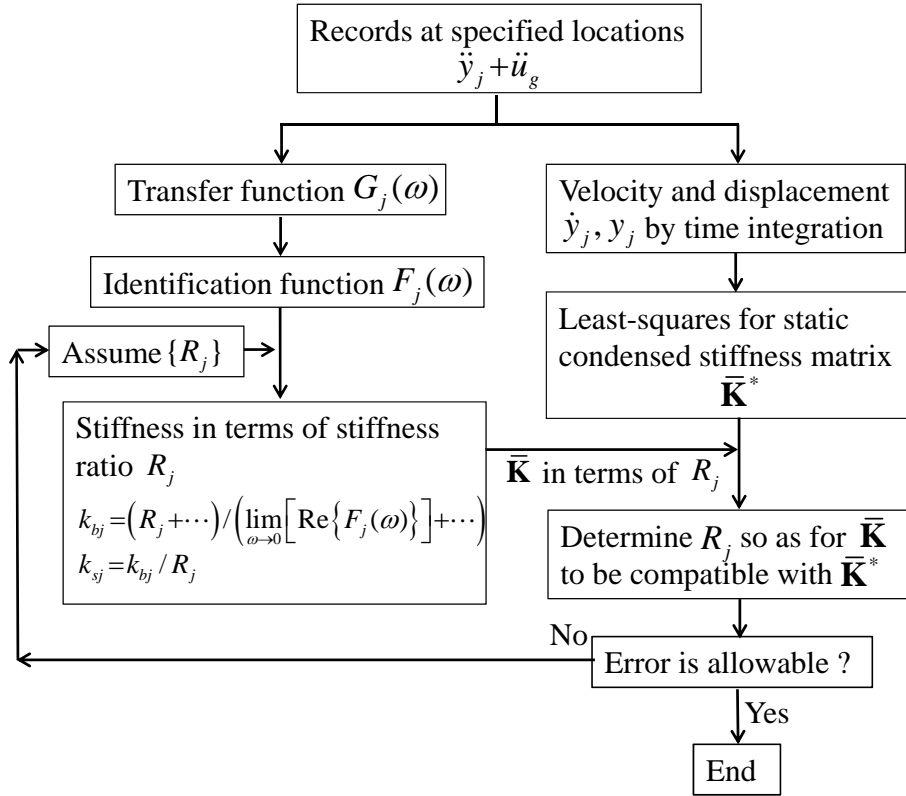


Fig.3 Flowchart of identification method 2

5. Addition of degrees of freedom

It is usual that the number of recording locations is very few. It is therefore difficult to express higher-mode effects in terms of a reduced model with masses at the recording points only. To overcome this difficulty, a technique is introduced such that some degrees of freedom are introduced between these recording points.

Consider an example as shown in Fig.4. Let \bar{G}_{2j-1} , \bar{G}_{2j} denote the transfer functions after the introduction of additional degrees of freedom. There is the following relation between \bar{G}_{2j-1} , \bar{G}_{2j} and G_j .

$$\bar{G}_{2j-1} \bar{G}_{2j} = G_j \quad (32)$$

Let introduce ratios α_j defined by

$$\lim_{\omega \rightarrow 0} \bar{G}_{2j} = \alpha_j \lim_{\omega \rightarrow 0} \bar{G}_{2j-1} \quad (33)$$

Then the newly defined transfer functions can be expressed in terms of the original transfer function and the ratios α_j .

$$\lim_{\omega \rightarrow 0} \bar{G}_{2j-1} = \sqrt{\left(\lim_{\omega \rightarrow 0} G_j \right) / \alpha_j} \quad (34a)$$

$$\lim_{\omega \rightarrow 0} \bar{G}_{2j} = \sqrt{\alpha_j \left(\lim_{\omega \rightarrow 0} G_j \right)} \quad (34b)$$

6. Identification of stiffness and damping coefficient using ARX model

In the previous method (Takewaki and Nakamura 2000, 2005) for shear building models, the limit manipulation of another identification function $f_j(\omega) = 1/F_j(\omega)$ for $\omega \rightarrow 0$ is used. However, it is often the case that the identification function becomes unstable and exhibits a large variability in the low frequency range. To overcome this difficulty, an ARX model is introduced which is a time-domain model. The reliability of the ARX model in this direction has been confirmed in the references (Takewaki and Nakamura 2009, Maeda et al. 2011). Especially, the applicability of the ARX model to shear building models has been demonstrated in the Reference (Maeda et al. 2011) and the applicability of the ARX model to shear-bending building models has been confirmed in the Reference (Kuwabara et al. 2012). It noted that Maeda et al. (2011) presented the relationships between the ARX parameters and the physical model parameters. This relationship enabled the reliable identification of physical parameters. In this regard, since it is useful to show the essence of the relation between the model stiffness and the ARX parameters, the limited summary of the Reference (Kuwabara et al. 2012) is shown in the following.

The following relation can be derived from the mechanical interpretation, i.e. the j -th floor and $(j-1)$ -th floor move identically at $\omega \rightarrow 0$.

$$\lim_{\omega \rightarrow 0} \operatorname{Re}\{G_j(\omega)\} = 1 \quad (35)$$

The following relation also holds because $G_j(\omega)$ should not include linear terms of ω .

$$\lim_{\omega \rightarrow 0} \frac{d}{d\omega} \operatorname{Im}\{G_j(\omega)\} = 0 \quad (36)$$

Consider the Taylor series expansion of $G_j(\omega)$ as follows.

$$G_j(\omega) = A_0 + A_1\omega + A_2\omega^2 + \dots \quad (37)$$

Equation (35) leads to Eq.(38) and Eq.(36) yields Eq.(39).

$$A_0^R = 1 \quad (38)$$

$$A_1^I = 0 \quad (39)$$

Since A_0^R and A_1^I are expressed in terms of the ARX parameters (Kuwabara et al. 2012), Eqs. 8) and (39) can be used to enhance the accuracy in the determination of the ARX parameters.

Let M_j denote $\sum_{i=j}^N m_i$. The stiffness can then be identified as

$$\lim_{\omega \rightarrow 0} \{ \text{Re}[1/f_j(\omega)] \} = \lim_{\omega \rightarrow 0} \{ \text{Re}[F_j(\omega)] \} = \frac{1}{k_{sj}} + \frac{H_j}{M_j} \sum_{m=1}^j \left[\frac{\sum_{i=m}^N \{ m_i (H_i^t - H_{m-1}^t) \}}{k_{bm}} \right] = \frac{A_2^R}{M_j} \quad (40)$$

Because A_2^R is also expressed in terms of the ARX parameters (Kuwabara et al. 2012), the stiffness identification problem can be reduced to the estimation problem of the ARX parameters. In other word, once the ARX parameters are obtained, the stiffness can be identified by using Eq.(40) and the assumed stiffness ratio.

It is important to investigate how to determine the number of order of the ARX model. Fig.4 shows an example of the correspondence of the function 'Fit' with the limit value at zero frequency of the real part of the identification function. The function Fit is defined by

$$\text{Fit} = \left(1 - \frac{\sqrt{\sum_{k=1}^{N_d} [\hat{y}(k) - y(k)]^2}}{\sqrt{\sum_{k=1}^{N_d} [y(k) - \bar{y}]^2}} \right) \times 100 [\%] \quad (41)$$

where $\hat{y}(k)$ denotes the data expressed by the ARX model and \bar{y} indicates the mean value.

The right ordinate in Fig indicates the limit value at zero frequency of the real part of the identification function.

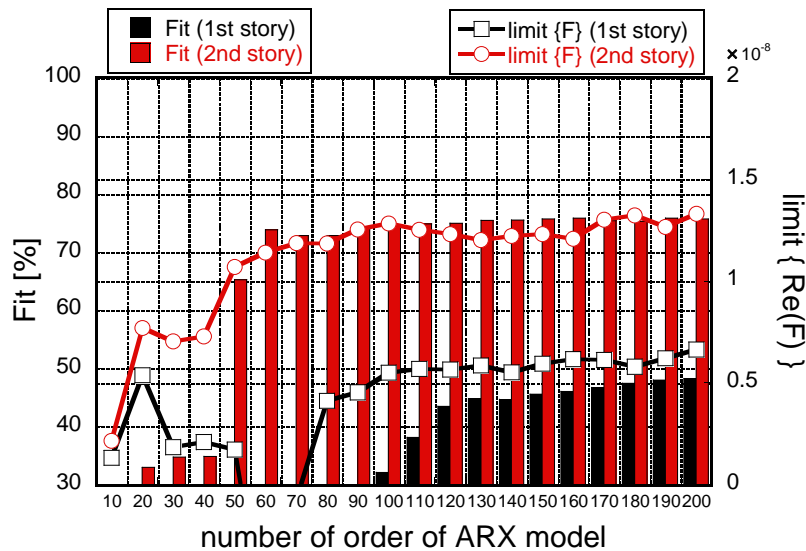


Fig.4 Determination of number of order of ARX model

7. Application of proposed identification methods to simulated data

In this section, the identification method 2 is applied to simulated data.

Consider a 60-story, 5-span planar steel frame, as shown in Fig.5, subjected to a ground motion recorded at the first floor of a super high-rise building in Shinjuku, Tokyo during the 2011 Tohoku earthquake. The length of every span is 10(m), every story height is 4(m), every floor mass is 2.56×10^5 [kg] and the common member Young's modulus is 2.05×10^5 [N/mm²]. The list of member cross-sections can be found in the Reference (Minami et al. 2012). It is known that this building was retrofitted several years ago using unique viscous oil dampers (avoiding excessive increase of force). It was reported that, while the top displacement reached 0.54(m), this building did not experience any damage during the 2011 Tohoku earthquake. Elastic time-history response analysis has been conducted using the frame model and the responses at representative points were employed as the substitution of recorded data. Model 1 (two points), 2 (three points), 3 (four points) as shown in Fig.6 have been used as the reduced shear-bending models. The stiffness-proportional damping is employed and the damping ratio is taken as 0.01 in accordance with the frame model. The transfer functions of these models and those of the corresponding shear models are shown in the Reference (Minami et al. 2012) together with those from the Fourier transform of the recorded data without and with the ARX model. The corresponding reduced shear model has been constructed by the procedure similar to the Reference (Takewaki and Nakamura 2000). The natural periods of lowest few modes of the shear-bending models and the shear models are presented in Tables 1 and 2. The top floor acceleration and displacement are shown in the Reference (Minami et al. 2012). It has been reported that the shear-bending model can simulate the response of the original frame more accurately than the reduced shear model. It has also been confirmed that the shear-bending model with more number of degrees of freedom can represent those of the original models with better accuracy.

Model 4 shown in Fig.6 is the model with two recording points and two additional

points. The method explained in Section 5 has been applied to Model 4. The comparison of the transfer functions has also been made in the Reference (Minami et al. 2012) among the reduced shear-bending and shear models and that from the records. The comparison of the first four natural periods among these models is also shown in Table 3. It has been confirmed that the shear-bending model with more number of degrees of freedom can represent the natural periods with better accuracy. The comparison of the lowest and second eigenmodes among models 1, 3, 4 and frame model can be found in the Reference (Minami et al. 2012). It has been confirmed that models 1, 3 and 4 can represent the eigenmodes up to the second within an acceptable accuracy. The comparison of the top story acceleration and displacement between the frame model (regarded as record) and the reduced models (shear-bending, shear: Model 4) can also be found in the Reference (Minami et al. 2012). It has been concluded that the shear-bending model can simulate the response of the original frame more accurately than the reduced two-mass model (Model 1).

A shear model without reduction is often used in the practical structural design of high-rise buildings. In order to investigate the accuracy of the proposed shear-bending model with few degrees of freedom, the comparison has been made in the Reference (Minami et al. 2012) of the top-story acceleration and displacement among the record, the reduced shear-bending model (Model 3) and the 60-mass shear model without reduction. Table 3 shows the first four natural periods of the 60-mass shear model. It has been reported (Minami et al. 2012) that the reduced shear-bending model (Model 3) can simulate the response of the original frame model more accurately than the 60-mass shear model especially in acceleration.

In order to investigate the usefulness of the proposed identification method and the obtained models, El Centro NS 1940 and Taft EW 1952 have been input to the frame model and the reduced models. The top-story acceleration and displacement have been compared in the Reference (Minami et al. 2012). It can be said that the reduced shear-bending model (Model 3) constructed by the proposed method using a set of vibration records for a specific ground motion can simulate the response (displacement at least) to other ground motions with a reasonable accuracy.

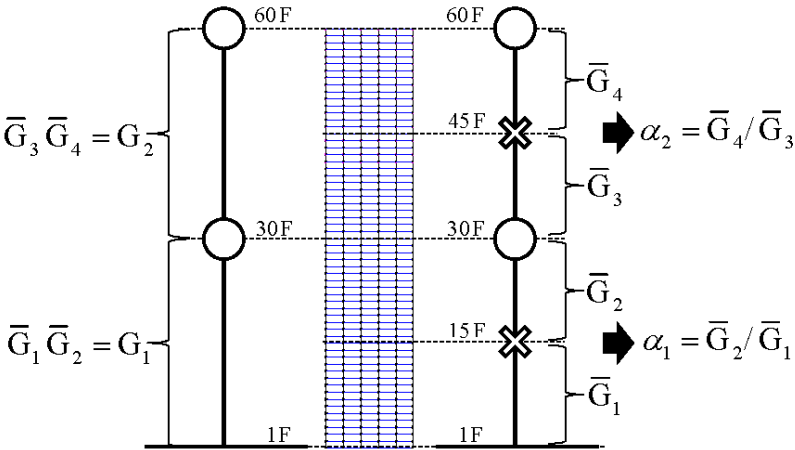


Fig.5 60-story, 5-span steel building frame and recording two points (two additional points are inserted)

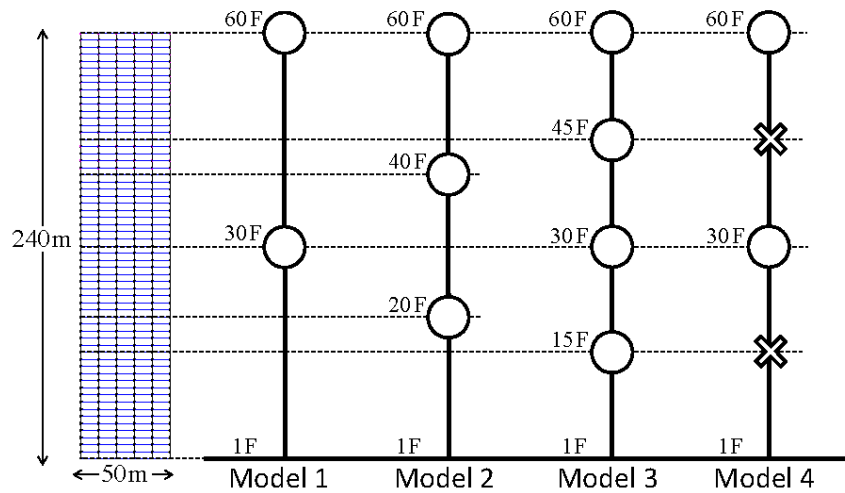


Fig.6 60-story, 5-span steel building frame and reduced models (Model 1-4)

Table 1 Natural periods (Model 1, 4)

Mod e no.	Original model [s]	Two-mass model (Model 1)		Extended 4-mass model (Model 4)	
		Shear-bending (error [%])	Shear (error)	Shear-bending (error [%])	Shear (error)
1	5.98	6.05 (1.2)	6.21 (3.8)	5.95 (-0.5)	6.00 (0.3)
2	1.98	1.93 (-2.5)	3.17 (60.3)	2.01 (0.5)	2.68 (35.3)
3	1.13			0.77 (-31.8)	2.03 (79.6)
4	0.81			0.68 (-16.0)	1.11 (37.0)

Table 2 Natural periods (Model 2, 3)

Mod e no.	Three-mass model (Model 2)		Four-mass model (Model 3)	
	Shear-bending [s] (error [%])	Shear (error)	Shear-bending (error [%])	Shear (error)
1	5.95 (-0.5)	6.04 (1.0)	5.95 (-0.4)	6.02 (0.6)
2	1.99 (0.6)	2.99 (51.0)	1.91 (-3.8)	2.75 (38.9)
3	1.31 (15.6)	1.80 (59.0)	1.42 (25.8)	1.91 (69.4)
4			0.94 (16.5)	1.17 (46.1)

Table 3 Natural periods (60-story shear model)

Mode no.	60-story shear model (error [%])
1	5.97 (0.02)
2	2.34 (18.2)
3	1.48 (31.0)
4	1.08 (33.3)

8. Application of proposed identification methods to actual buildings

In this section the identification method 1 is applied after the application of the identification method 2. This is because, while the identification method 1 is more accurate than the identification method 2 and sensitive to the initial guess of parameters, the identification method 2 is more robust to the initial guess of parameters. In the identification method 1 used after the application of the identification method 2, the natural periods are determined so that both transfer functions between the measured data and the identification model are compatible.

The most devastating earthquake in Japan after the 1923 Great Kanto earthquake occurred on March 11, 2011. The moment magnitude was 9.0 and this is the largest so far in Japan. The earthquake resulted from the thrust faulting near the subduction zone plate boundary between the Pacific and North America Plates. Nearly 20,000 people were killed or are still missing by that earthquake and the subsequent monster tsunami. Because super high-rise buildings in mega cities in Japan had never been shaken intensively by the so-called long-period ground motions before March 11, 2011, the response of high-rise buildings to such long-period ground motions is one of the most controversial subjects and issues in the field of earthquake-resistant design in Japan.

The proposed identification methods are applied to two actual super high-rise buildings in Japan which were shaken during the 2011 Tohoku earthquake.

8.1 Application to super high-rise building in Osaka bay area

The first actual example is the super high-rise building in Osaka bay area shown in Fig.7 (Takewaki et al. 2011a, 2012, 2013a, Celebi et al. 2012). This building is a 55-story super high-rise steel building frame (height=256m: fundamental natural period=5.8s (long-span direction), 5.3s (short-span direction)). It is unusual in Japan that these detailed structural design data are available. This building is reported to have been shaken severely regardless of the fact that Osaka is located far from the epicenter (about 800km) and the JMA instrumental intensity was 3 in Osaka. It should be pointed out that the level of velocity response spectra of ground motions observed here (first floor) is almost the same as that at the Shinjuku station (K-NET) in Tokyo and the top-story displacement are about 1.4m (short-span direction) and 0.9m (long-span direction). Fig.8 shows the response amplification observed in this building during the 2011 Tohoku earthquake.

Table 4 shows the comparison of natural periods of the original building model (obtained from records) and the reduced shear-bending and shear models in the short-span direction. It can be observed that the shear-bending model can represent the second and third-mode natural periods more accurately than the shear model. Fig.9 illustrates the top-story accelerations and displacements of the reduced shear-bending and shear models together with the records. In this analysis, the stiffness-proportional damping is used and the damping ratio is taken as 0.015 judging from the compatibility in transfer functions between the measured data and the identified one. Since this building is just resonant with the surface ground fundamental natural period of about 6.5s as is well-known, the fundamental-mode vibration component is predominant. For this reason both the reduced shear-bending and shear models can simulate the

top-story acceleration and displacement within an acceptable accuracy.

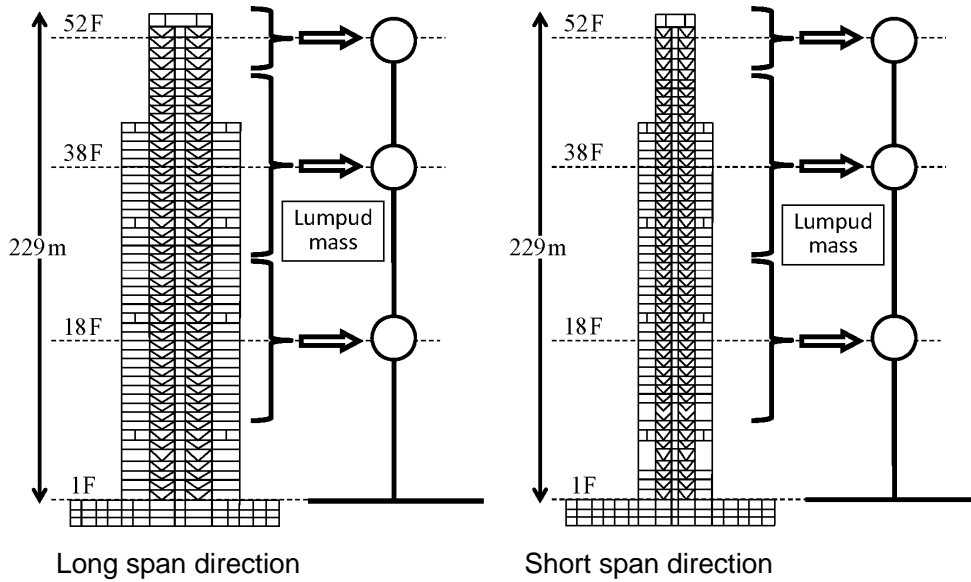
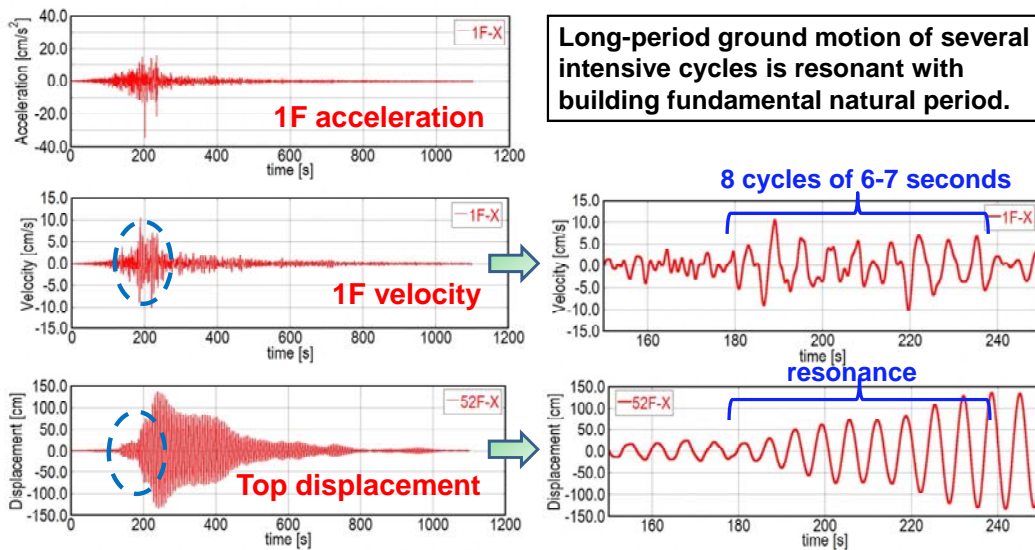


Fig.7 Super high-rise building at Osaka bay area



Long-period ground motion of several intensive cycles is resonant with building fundamental natural period.

Fig.8 Ground acceleration, velocity and top-story displacement (short span direction): Reality of resonance in a 55-story building in Osaka

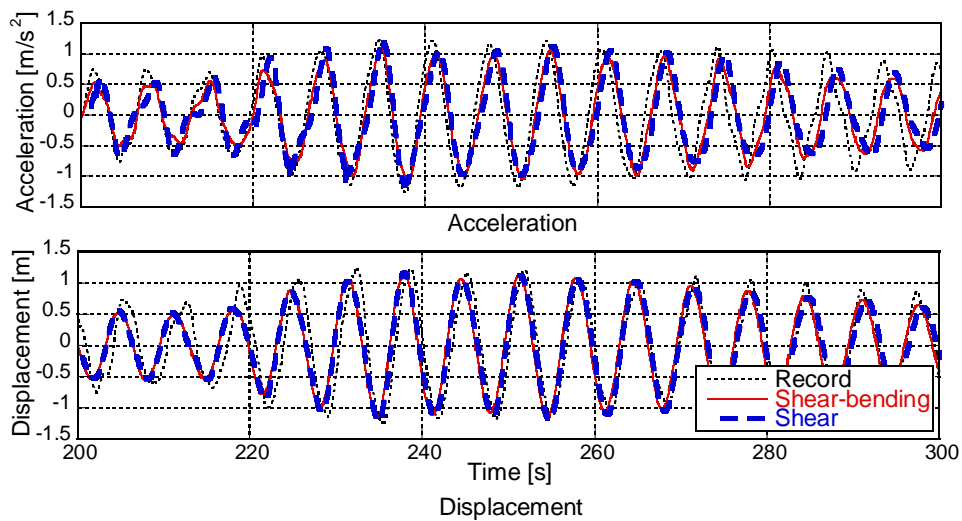


Fig.9 Comparison among record, identified response by shear-bending model and that by shear model (Short span direction)

Table 4 Comparison of modeling accuracy in terms of natural periods (Short span direction)

Mode	Model from records [s]	Shear bending (error [%])	Shear (error [%])
1	6.55	6.64 (1.3)	6.67 (1.9)
2	2.08	2.09 (0.4)	3.26 (56.7)
3	1.11	1.33 (20.1)	1.70 (53.6)

8.2 Application to super high-rise building in Shinjuku, Tokyo

The second actual example is the super high-rise building in Shinjuku, Tokyo as shown in Fig.10. This building is a 54-story steel building frame (height=223m: fundamental natural period=6.2s (short-span direction of 42m), 5.2s (long-span direction of 63m)) retrofitted with nonlinear oil dampers including the supporting bracing system. This building experienced a top displacement of 0.54(m) during the 2011 Tohoku earthquake. The vibration duration has been reported to be over 13 minutes. It has also been reported that the building would have attained a top displacement of 0.7(m) if the passive dampers had not been installed.

Table 5 presents the comparison of natural periods of the original building model (obtained from records) and the reduced shear-bending and shear models in the short-span direction. Since the floor mass distribution is not known, an ordinary floor mass of 1.0×10^3 (kg/m²) is assumed. It can be observed that the shear-bending model can represent the second-mode natural period more accurately than the shear model. Fig.11 shows the comparison of top-story accelerations and displacements in the short-span direction. In this analysis, the stiffness-proportional damping is used and the damping ratio is taken as 0.027 (short-span direction) judging from the compatibility in transfer functions between the measured data and the identified one. It can be found

that both the reduced shear-bending and shear models cannot simulate the actual response within an acceptable level. Uncertain factors are (i) the distribution of floor masses, (ii) the structural damping model (stiffness-proportional one was used), (iii) the effect of nonlinear viscous dampers and (iv) restriction of degrees of freedom of the reduced model.

To investigate the performance of the technique explained in Section 5, additional two points (mid-point between the original points) are inserted in the two-mass reduced model (see Fig.10(b)). The Rayleigh damping model is used and the first and second-mode damping ratios are taken as 0.027 and 0.024 in the short-span direction judging from the compatibility in transfer functions between the measured data and the identified one. The comparison has been made in the Reference (Minami et al. 2012) of natural periods of the original building model (obtained from records) and the reduced shear-bending and shear models. It has been observed that the extended shear-bending model can represent the second and third-mode natural periods more accurately than the shear model. It has also been seen that the extended shear-bending model can represent the higher-mode effect more clearly in acceleration. It has been confirmed that the technique of expansion of degrees explained in Section 5 is promising.

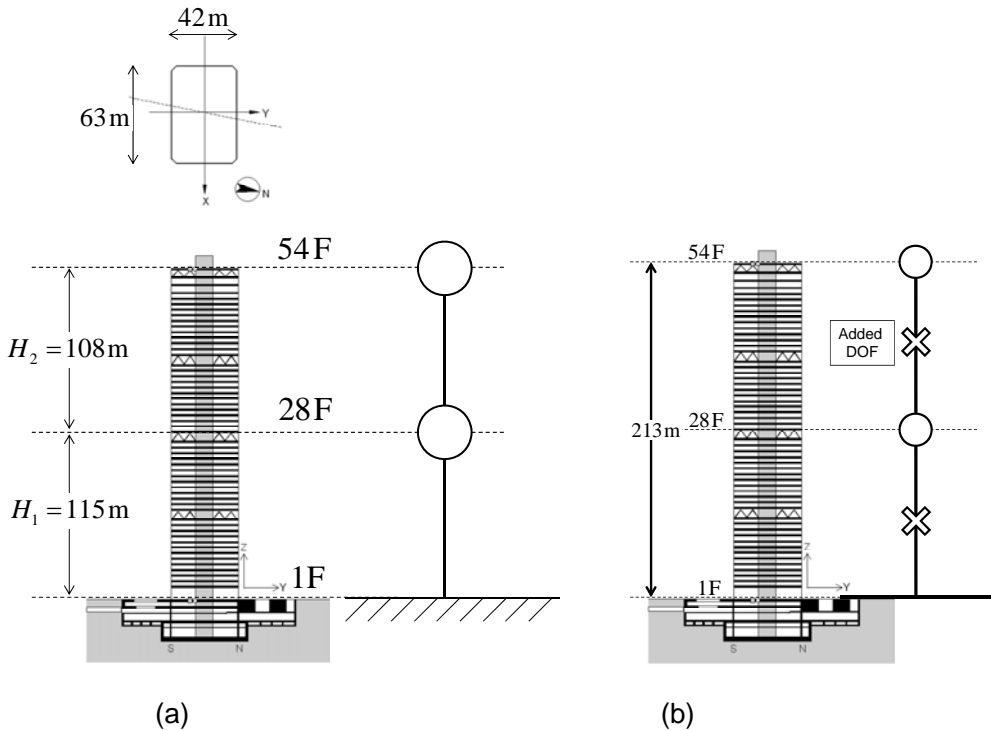


Fig.10 Super high-rise building at Shinjuku, Tokyo

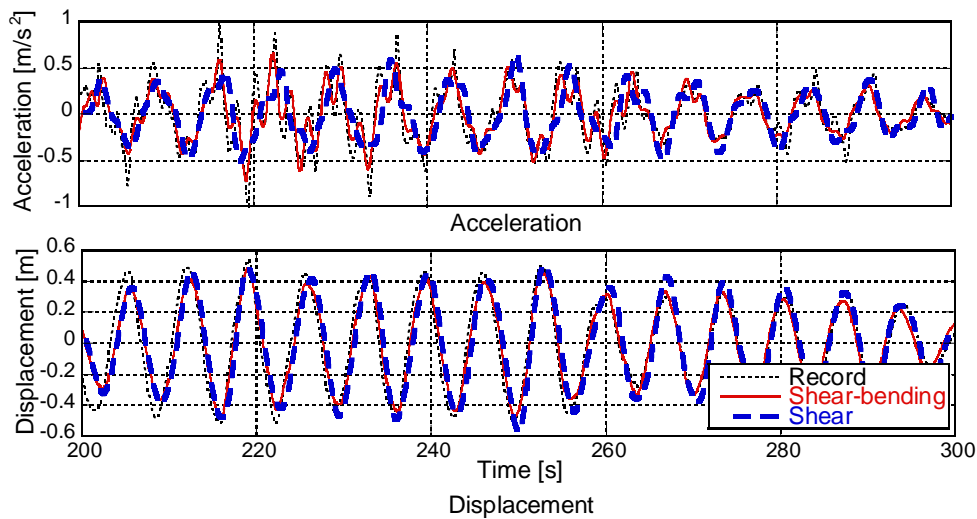


Fig.11 Comparison among record, identified response by shear-bending model (model with added degrees of freedom) and that by shear model (model with added degrees of freedom)

Table 5 Comparison of modeling accuracy in terms of natural periods

Mode	Model from records [s]	Shear bending (error [%])	Shear (error [%])
1	6.50	6.64 (2.2)	6.69 (2.9)
2	2.01	2.02 (0.3)	3.05 (51.7)
3	1.04	1.29 (23.6)	2.06 (97.8)
4	—	1.06 (—)	1.49 (—)

9. Time-varying identification

In the previous sections, the batch least-squares method has been used in which the total duration is employed as the duration for estimating a set of ARX parameters. In other words, averaged values of ARX parameters in the total time duration have been evaluated.

It is well known that the natural period of buildings depends on the amplitude of vibration and some parts in the super high-rise building at Osaka bay area (Fig.7) experienced a limited amount of non-structural damage.

In order to investigate the time-varying mechanical characteristics of a building, a new time-varying identification method is proposed. This method was first proposed by Takewaki and Nakamura (2009) for a shear building model. In this paper, this method is extended to a shear-bending model and stiffnesses are also identified in addition to the natural period and damping ratio.

30 seconds were used as the evaluation time for the batch least-squares method and this process was repeated by moving 1 second later.

Fig.12 shows the top-story displacement of the super high-rise building at Osaka bay

area (Fig.7) and the corresponding identified fundamental natural period (Takewaki et al. 2013b). It can be observed that a slight elongation of the fundamental natural period corresponds fairly well with the large displacement amplitude.

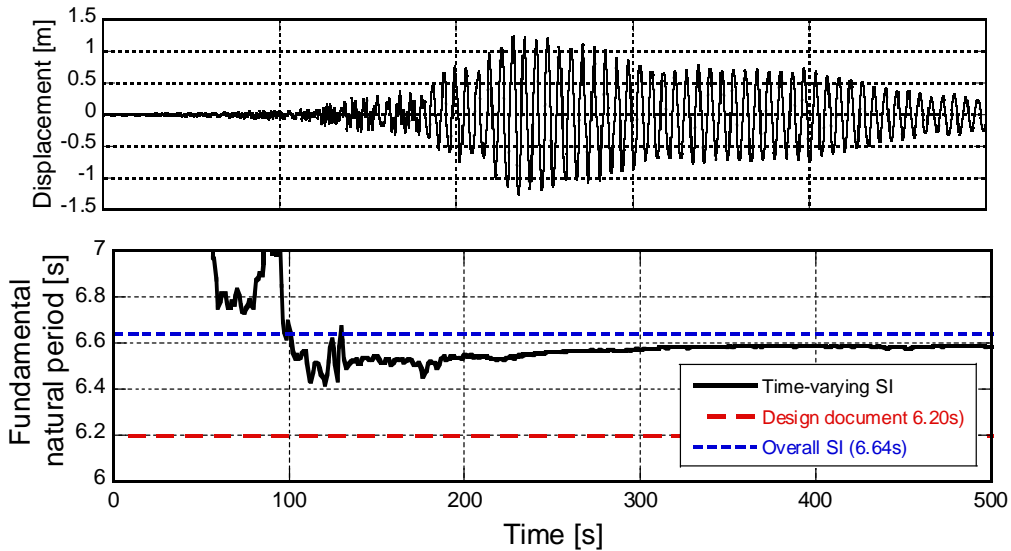


Fig.12 Top-story displacement and fundamental natural period of super high-rise building at Osaka bay area

Fig.13 indicates the top-story displacement of the super high-rise building at Shinjuku, Tokyo (Fig.10) and the corresponding identified fundamental natural period (Takewaki et al. 2013b). A slight elongation of the fundamental natural period can be seen with the appearance of the large displacement amplitude. As for this building, several data on the fundamental natural period are available and these values are shown in Fig.13.

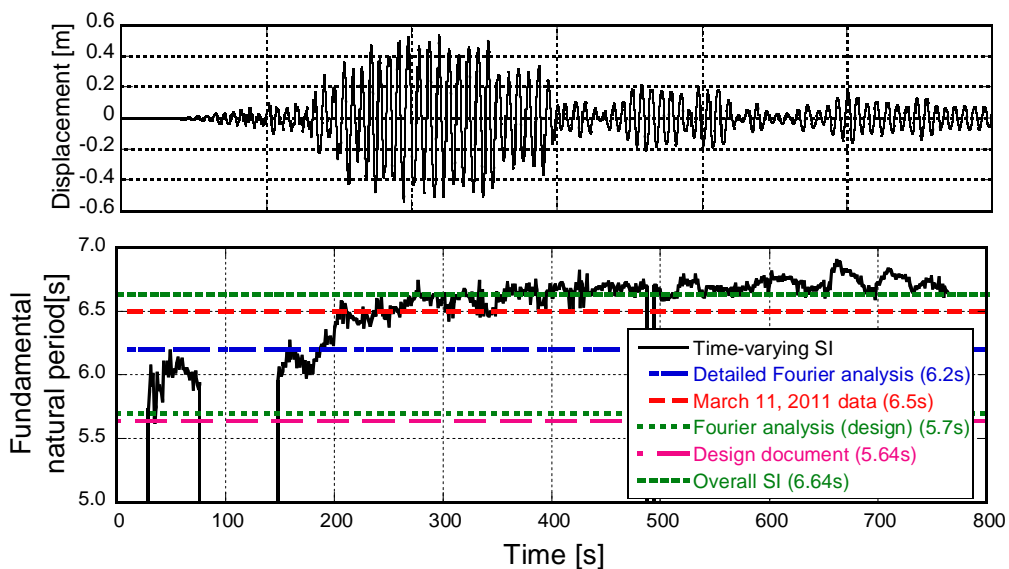


Fig.13 Top-story displacement and fundamental natural period of super high-rise building at Shinjuku, Tokyo

10. Conclusions

A new method of system identification of high-rise buildings has been proposed which uses a shear-bending model. Two major difficulties have been overcome, i.e. (i) the specification of shear-bending ratios in high-rise buildings and (ii) the identification from limited observation (usually a few records in a building). The principal results may be summarized as follows.

- (1) A difficulty in the previous work (Kuwabara et al. 2012) in the specification of shear-bending ratios in a shear-bending model for high-rise buildings has been overcome by selecting such ratios as unknown parameters. Such unknown parameters have been determined by fitting the transfer functions or minimizing un-equilibrium forces acting on floors. The proposed identification method takes full advantage of the limit value of an identification function at zero frequency which includes the transfer function.
- (2) An identification method (method 1) has been proposed which is based on the fitting of the transfer functions between one constructed for the model including unknown shear-bending ratios and the other one constructed directly from the records.
- (3) Another identification method (method 2) has been proposed which is based on the minimization of un-equilibrium forces between two ones described just above.
- (4) A technique of adding degrees of freedom between the recording locations is effective for the enhancement of accuracy of the proposed identification methods.
- (5) The proposed shear-bending model can represent higher-mode natural periods of the original model in a more accurate way than the corresponding shear building model.
- (6) An ARX model is shown to be useful for reliable and accurate identification. Unstable properties of the identification function have been eliminated.
- (7) It has been demonstrated through the application to actual data recorded in super high-rise buildings during the 2011 off the Pacific coast of Tohoku earthquake that the repetitive application of the proposed two identification algorithms can enhance the reliability and accuracy of the proposed identification method.
- (8) The time-varying identification of modal parameters (fundamental natural period, lowest-mode damping ratio, story stiffnesses) can be conducted by setting an appropriate duration of evaluation in the batch least-squares method.

Acknowledgements

The author would like to thank Mr.Y.Minami and Ms.A.Ikeda for their help in the computation. Part of the present work is supported by the Grant-in-Aid for Scientific Research of Japan Society for the Promotion of Science (No.21360267, 23656340, 24246095). This support is greatly appreciated. The use of ground motion records from Building Research Institute of Japan, Osaka Prefectural Office and Taisei Co. is also appreciated.

References

- Agbabian M.S, Masri S.F., Miller R.K. and Caughey T.K. (1991). System identification approach to detection of structural changes, *J. Engng. Mech.*, ASCE; **117**(2): 370-390.
- Barroso L. R., and Rodriguez R. (2004). Damage detection utilizing the damage index method to a benchmark structure. *J. Engng. Mech.*, ASCE; **130**(2): 142–151.
- Beck, JL(1996). System identification methods applied to measured seismic response, *Proc. 11th World Conf. Earthq. Eng.*, Paper No.2004.
- Beck J.L. and Jennings P.C. (1980). Structural identification using linear models and earthquake records, *Earthquake Engng. Struct. Dyn.*; **8**: 145-160.
- Bernal D. and Beck J. (2004). Preface to the Special Issue on Phase I of the IASC-ASCE Structural Health Monitoring Benchmark, *J. Engng. Mech.*, ASCE; **130**(1): 1-2.
- Casciati F. (ed.) (2002). *Proceedings of 3rd World Conference on Structural Control*. John Wiley & Sons: Como.
- Celebi, M. (1996). Comparison of damping in buildings under low-amplitude and strong motions. *J. Wing. Eng. & Ind. Appl.*; **59**(2-3): 309-323.
- Celebi, M., Okawa, I., Kashima, T., Koyama, S. and Iba, M. (2012). Response of a tall building far from the epicenter of the 11 March 2011 M9.0 Great East Japan earthquake and aftershocks, *Struct. Design Tall Spec. Build.* (published online).
- Doebling S.W., Farrar C.R., Prime M.B. and Shevitz D.W. (1996) *Damage identification and health monitoring of structural and mechanical systems from changes in their vibration characteristics: A literature review*, Los Alamos National Laboratory Report LA-13070-MS.
- Dunand, F., Gueguen, P., Bard, P-Y, Rodgers, J. and Celebi, M. (2006). Comparison of the dynamic parameters extracted from weak, moderate and strong building motion. *Proc. 1st European Conf. of Earthq. Eng. and Seismology*, Geneva, Switzerland, paper 1021.
- Fujino, Y., Nishitani, A. and Mita, A. (2010). *Proceedings of 5th World Conference on Structural Control and Monitoring, (5WCSCM)*. Tokyo.
- Ghanem R. and Shinozuka M. (1995). Structural-system identification I: Theory, *J. Engng. Mech.*, ASCE; **121**(2): 255-264.
- Goel, R.K. (2008). Mode-based procedure to interpolate strong motion records of instrumented buildings, *ISET J. Earthquake Technology*; **45**(3-4): 97–113.
- Hart G.C. and Yao J.T.P. (1977). System identification in structural dynamics, *J. Engng. Mech. Div.*, ASCE; **103**(EM6): 1089-1104.
- Heredia-Zavoni E and Esteva L (1998).. Optimal instrumentation of uncertain structural systems subject to earthquake ground motions. *Earthquake Engng. Struct. Dyn.*; **27**:343–362.
- Hernandez-Garcia, M.R., Masri, S.F., Ghanem, R., Figueiredo, E., and Farrar, C.R. (2010a). An experimental investigation of change detection in uncertain chain-like systems. *J. Sound Vib.*, 2010; **329**(12):2395–2409.
- Hernandez-Garcia, M., Masri, S.F., Ghanem, R., Figueiredo, E., Farrar, R.A. (2010b). A structural decomposition approach for detecting, locating, and quantifying nonlinearities in chain-like systems. *Struct. Control Health Monitoring*, **17**(7),

- 761-777, 2010.
- Hisada, Y., Yamashita, T., Murakami, M., Kubo, T., Shindo, J., Aizawa, K. and Arata, T. (2012). Seismic response and damage of high-rise buildings in Tokyo, Japan, during the Great East Japan earthquake, *Proc. Int. Symp. on Engineering Lessons Learned from the 2011 Great East Japan Earthquake*, March 1-4, 2012, Tokyo, Japan, pp1110-1119.
- Hjelmstad K.D, Banan Mo.R and Banan Ma.R. (1995). On building finite element models of structures from modal response, *Earthquake Engng. Struct. Dyn.*; **24**: 53-67.
- Hjelmstad K.D. (1996). On the uniqueness of modal parameter estimation, *J. Sound and Vib.* **192**(2): 581-598.
- Hoshiya M. and Saito E (1984).. Structural identification by extended Kalman filter, *J. Engng. Mech.*, ASCE; **110**(12): 1757-1770.
- Housner GW, Masri SF, Chassiakos AG. (eds). (1994). *Proceedings of 1st World Conference on Structural Control*. IASC: Los Angeles, CA.
- Housner G., Bergman, L.A., Caughey, T.K., Chassiakos, A.G., Claus, R.O., Masri, S.F., Skelton, R.E., Soong, T.T., Spencer, B.F. and Yao, J.T.P. (1997). Special issue, Structural control: past, present, and future, *J. Engng. Mech.*, ASCE; **123**(9): 897-971.
- Ji X., Fenves GL, Kajiwara K, and Nakashima M. (2011). Seismic damage detection of a full-scale shaking table test structure, *J. Struct. Engng.* ASCE; **137**(1): 14-21.
- Johnson E., and Smyth A. (eds). (2006). *Proceedings of 4th World Conference on Structural Control and Monitoring, (4WCSCM)*. IASC: San Diego, CA.
- Kasai, K., Pu, W. and Wada, A. (2012). Responses of controlled tall buildings in Tokyo subjected to the Great East Japan earthquake, *Proc. Int. Symp. on Engineering Lessons Learned from the 2011 Great East Japan Earthquake*, March 1-4, 2012, Tokyo, Japan, pp1099-1109.
- Kerschen, G., Worden, K., Vakakis, A.F. & Golinval, J.-C. (2006). Past, present and future of nonlinear system identification in structural dynamics, *Mech. Syst. Signal Process.*, **20**, 505–592.
- Kobori T, Inoue Y, Seto K, Iemura H and Nishitani A. (eds). (1998). *Proceedings of 2nd World Conference on Structural Control*. John Wiley & Sons: Kyoto.
- Kozin F. and Natke H.G. (1986). System identification techniques, *Struct. Safety*, **3**: 269-316.
- Koh C.G., See L.M and Balendra T. (1991). Estimation of structural parameters in time domain: a substructure approach, *Earthquake Engng. Struct. Dyn.*; **20**: 787-801.
- Kuwabara, M., Yoshitomi, S. and Takewaki, I. (2012). A new approach to system identification and damage detection of high-rise buildings, *Struct. Control Health Monitoring*, **20**(5), 703-727.
- Lee, Y.S., Vakakis, A.F., McFarland, D.M. and Bergman, L.A. (2010). A global–local approach to nonlinear system identification: A review, *Struct. Control Health Monitoring*, **17**(7), 742-760.
- Limongelli, M.P. (2003). Optimal location of sensors for reconstruction of seismic responses through spline function interpolation, *Earthquake Engng. Struct. Dyn.*; **32**(7): 1055–1074.
- Limongelli, M.P. (2005). Performance evaluation of instrumented buildings, *ISSET Journal of Earthquake Technology*, **42**(2-3): 47–61.

- Lus, H., Betti, R and Longman, RW. (1999). Identification of linear structural systems using earthquake induced vibration data, *Earthq. Eng. Struct. Dyn.*; **28**: 1449-1467.
- Lus H., Betti R., Yu J., and De Angelis M. (2004). Investigation of a system identification methodology in the context of the ASCE benchmark problem, *J. Engng. Mech.*, ASCE; **130**(1): 71-84.
- Maeda T., Yoshitomi S. and Takewaki I. (2011). Stiffness-damping identification of buildings using limited earthquake records and ARX model, *J. Struct. Construction Eng.*, Architectural Inst. of Japan; **666**: 1415-1423 (in Japanese).
- Masri S.F., Nakamura M., Chassiakos A.G. and Caughey T.K. (1996). A neural network approach to the detection of changes in structural parameters, *J. Engng. Mech.*, ASCE; **122**(4): 350-360.
- Minami, Y., Yoshitomi, S. and Takewaki, I. (2012). System identification of super high-rise buildings using limited vibration data during the 2011 Tohoku (Japan) earthquake, *Structural Control and Health Monitoring* (Published online).
- Naeim, F. (2000). Learning from structural and nonstructural seismic performance of 20 extensively instrumented buildings, *Proc. 12th World Conf. Earthq. Eng.*, Paper No.2004.
- Nagarajaiah, S., and Basu, B. (2009). Output only modal identification and structural damage detection using time frequency & wavelet techniques, *Earthquake Engng. Engng. Vib*; **8**(4): 583-605.
- Nayeri, R.D., Masri, S.F., Ghanem, R.G. and Nigbor, R.L. (2008). A novel approach for the structural identification and monitoring of a full-scale 17-story building based on ambient vibration measurements, *Smart Materials and Structures*; **17**(2): 1-19.
- Papadimitriou, C. (2004). Optimal sensor placement methodology for parametric identification of structural systems, *J. Sound Vib.*; **278**(4-5): 923–947.
- Safak, E. (1995). Detection and identification of soil-structure interaction in buildings from vibration recordings. *J. Struct. Eng.* ASCE; **121**(5): 899-906.
- Safak E. (1989). Adaptive modeling, identification, and control of dynamic structural systems. I: Theory, *J. Engng. Mech.*, ASCE; **115**(11): 2386-2405.
- Shah PC and Udawadia FE (1978). A methodology for optimal sensor locations for identification of dynamic systems. *J. Applied Mech.*, ASME; **45**:188 –196.
- Shinozuka M. and Ghanem R. (1995). Structural-system identification II: Experimental verification, *J. Engng. Mech.*, ASCE; **121**(2): 265-273.
- Stewart, JP and Fenves, GL. (1998). System identification for evaluating soil-structure interaction effects in buildings from strong motion recordings, *Earthq. Eng. Struct. Dyn.*; **27**(8): 869-885.
- Takewaki I. and Nakamura M. (2000). Stiffness-damping simultaneous identification using limited earthquake records, *Earthquake Engng. Struct. Dyn.*; **29**(8): 1219-1238.
- Takewaki I., and Nakamura M. (2005). Stiffness-damping simultaneous identification under limited observation, *J. Engng. Mech.*, ASCE; **131**(10): 1027-1035.
- Takewaki, I., Murakami, S., Fujita, K., Yoshitomi, S., and Tsuji, M. (2011a). The 2011 off the Pacific coast of Tohoku earthquake and response of high-rise buildings under long-period ground motions, *Soil Dyn. Earthq. Engng.*; **31**(11): 1511-1528.
- Takewaki, I., Nakamura, M. and Yoshitomi, S. (2011b). *System identification for structural health monitoring*, WIT Press (UK).

- Takewaki I. and Nakamura M. (2009). Temporal variation of modal properties of a base-isolated building during an earthquake, *J. Zhejiang University-SCIENCE A*; **11**(1): 1-8.
- Takewaki, I., Moustafa, A. and Fujita, K. (2012). *Improving the Earthquake Resilience of Buildings: The worst case approach*, Springer (London) (ISBN-10: 1447141431, ISBN-13: 978-1447141433).
- Takewaki, I., Fujita, K. and Yoshitomi, S. (2013a). Uncertainties in long-period ground motion and its impact on building structural design: Case study of the 2011 Tohoku (Japan) earthquake, *Engineering Structures*, **49**, 119-134.
- Takewaki, I., Minami, Y., Ikeda, A. and Fujita, K. (2013b). System identification of super high-rise buildings using limited vibration data during the 2011 Tohoku earthquake, *Proc. of Two Year Memorial Symposium after 2011 Great East Japan Earthquake*, March 27-29, 2013, Tokyo, pp313-314.
- Udwadia F.E., Sharma D.K and Shah P.C. (1978). Uniqueness of damping and stiffness distributions in the identification of soil and structural systems, *J. Applied Mech.*, ASME; **45**: 181-187.
- Udwadia FE. (1994). Methodology for optimum sensor locations for parameter identification in dynamic systems. *J. Engng. Mech.*, ASCE; **120**:368 –390.
- Worden, K. and Burrows, A.P., Optimal sensor placement for fault detection, *Engineering Structures* 2001; **23**(8): 885–901.
- Yang, Y. and Nagarajaiah, S. (2012). Time-frequency blind source separation using independent component analysis for output-only modal identification of highly-damped structures, *J. Struct. Eng.* ASCE 2012, doi:10.1061/(ASCE)ST.1943-541X.0000621 (accepted for publication).
- Yao J.T.P. and Natke H.G. (1994). Damage detection and reliability evaluation of existing structures, *Struct. Safety*, **15**: 3-16.
- Yi, T.-H., Li, H.-N. and Gu, M. (2011). A new method for optimal selection of sensor location on a high-rise building using simplified finite element model, *Struct. Engng Mech.*; **37**(6): 671-684.
- Yoshitomi, S., Kuwabara, M., Tsuji, M. and Takewaki, I. (2010). Stiffness and damping simultaneous identification based on extrapolation of unrecorded response to ground motion, *Proc. of The First Int Conf. on Advances in Interaction and Multiscale Mechanics (AIMM'10)*, 30 May - 4 June 2010 in Jeju, Korea, pp330-349.